ISBN: 978-90-75815-17-7 and 978-1-4799-0114-2

Proceedings of the European Conference on Power Electronics and Applications (EPE, ECCE Europe), Lille, France, 3-5 September, 2013.

# Mission Profile based Multi-Disciplinary Analysis of Power Modules in Single-Phase Transformerless Photovoltaic Inverters

Yongheng Yang
Huai Wang
Frede Blaabjerg
Ke Ma

## Suggested Citation

Y. Yang, H. Wang, F. Blaabjerg, and K. Ma, " Mission profile based multi-disciplinary analysis of power modules in single-phase transformerless photovoltaic inverters," *in Proc. European Conference on Power Electronics and Applications (EPE).*, 2013, pp. P.1-P.10.

# Mission Profile based Multi-Disciplinary Analysis of Power Modules in Single-Phase Transformerless Photovoltaic Inverters

Yongheng Yang, Huai Wang, Frede Blaabjerg, Ke Ma
Department of Energy Technology, Aalborg University
Pontoppidanstraede 101, DK-9220 Aalborg East
Aalborg, Denmark
Tel.: +45 / 99 40 97 66
Fax: +45 / 98 15 14 11
E-Mail: yoy@et.aau.dk, hwa@et.aau.dk, fbl@et.aau.dk, kema@et.aau.dk
URL: http://www.et.aau.dk

## Acknowledgements

The authors would like to thank China Scholarship Council (CSC) and the Department of Energy Technology at Aalborg University for supporting this PhD project.

## Keywords

«Mission profile», «Thermal stress», «Reliability», «Photovoltaic», «Single phase system», «Voltage source converter»

## Abstract

The popularity of transformerless photovoltaic (PV) inverters in Europe proves that these topologies can achieve higher efficiency (e.g., ≥ 98% has been reported). Along with the advanced power electronics technology and the booming development of PV power systems, a long service time (e.g. 25 years) has been set as a main target and an emerging demand from the customers, which imposes a new challenge on grid-connected transformerless inverters. In order to reduce maintenance cost, it is essential to predict the lifetime of the transformerless PV inverter and its components based on the mission profiles – solar irradiance and ambient temperature. In this paper, a mission profile based analysis approach is proposed and it is demonstrated by three main single-phase transformerless PV inverters - Full-Bridge (FB) with bipolar modulation scheme, the FB inverter with DC bypass (FB-DCBP) topology and the FB inverter with AC bypass leg (highly efficient and reliable inverter concept, HERIC inverter). Since the thermal stress is one of the most critical factors that induce failures, the junction temperatures on the power devices of the three topologies are analyzed and compared by considering the mission profiles. The lifetimes of these topologies are discussed according to the thermal performance and the power losses on the switching devices are also compared.

## Introduction

The development of single-phase photovoltaic (PV) power systems connected to the grid has been booming progressively in recent years due to the matured PV technology, the continuous declined price of PV panels[1]-[7]. The penetration level of PV power systems is going to be much higher with the increasing demand for environmental-friendly electricity generation. However, when this comes into reality, the high grid-integration level will introduce negative impacts on the public network, making the grid much more uncontrollable and heterogeneous [4], [5]. Such concerns like efficiency and emerging reliability are becoming of high interest in order to reduce energy losses and maintenance cost, and extend the service time. Underpinned by appropriate control methods and advanced power electronics technology (e.g. PV inverters), transformerless inverters are increasingly in popularity in European and Australian markets since they can achieve higher efficiency, lower weight and cheaper cost compared to traditional transformer-based PV power systems.

However, the removal of transformers may cause safety problem because of the loss of galvanic isolation between the grid and the PV inverters [8], [9]. Consequently, several transformerless topologies are

proposed to solve this issue by means of disconnecting the PV array from the grid [8]-[15]. This can be done either on the DC-side of the inverter (FB-DCBP inverters [11], [12]) or on the AC-side (HERIC inverter patented by Sunways [13]). By doing so, both the switches and the output inductors are subject to half of the input voltage stress, leading to high efficiency, when the zero voltage state is applied to the grid. Those transformerless inverters require additional power switches to realize the disconnection of the PV panels from the grid.

Apart from high efficiency, recently, achieving high reliability in the power devices is becoming a must for the design and operation of PV power systems [16]-[33]. According to a 5-year field experience in a large utility-scale PV generation plant presented in [16], the PV inverters are responsible for 37% of the unscheduled maintenance and 59% of the associated cost for the maintenance. As the essential interface components for PV panels and the grid, the power electronics devices/systems (e.g. transformerless PV inverters) are one of the lifetime limiting and the most vulnerable parts in the entire PV systems as presented in [4], [5], [17]-[27]. Various factors, like temperature, humidity, electrical overstress and severe users, can induce the failures of PV inverters [29]. Besides these factors under normal operations, failures are more prone to occur under non-intentional operations in islanding mode or under grid faults [31].

Among those factors, the most observed factors that cause failures are related to the temperature, including mean junction temperature and temperature swings [18], [19], [32]. As it is aforementioned, in different transformerless topologies, additional power devices are required to achieve high efficiency. Those power devices will inevitably cause a redistribution of the power losses on the PV inverter, especially by considering a certain application where the solar irradiance and ambient temperature are not constant. Since the thermal distribution and the loss distribution inside the PV inverters are related to the reliability, the redistribution of power losses will affect the system reliability. Thus, the knowledge of the mission profile (solar irradiance and ambient temperature) is crucial for the reliability evaluation and further optimized design of power electronics in PV inverters [4], [17]-[19], [23].

By considering the above issues, a multi-disciplinary analysis and evaluation method is proposed in § II in this paper. It is followed by the modelling of the mainstream transformerless topologies- Full-Bridge (FB) with bipolar modulation scheme, the FB inverter with DC bypass (FB-DCBP) topology and the FB inverter with AC bypass leg (Highly Efficient and Reliable Inverter Concept, HERIC). To demonstrate the proposed method, a 3 kW single-phase grid-connected system is firstly examined in a constant operation condition (solar irradiance: 1000 W/m$^2$, ambient temperature: 50 °C) and then it is tested with real mission profiles (yearly data at Aalborg University from Oct. 2011 to Sept. 2012). Based on the results, the lifetimes of the three topologies can be calculated and compared by means of rain-flow analysis, and the energy yield can qualitatively be estimated. Finally, conclusions are drawn.

## Mission Profile based Multi-Disciplinary Analysis Method

With the accumulative field experience and the introduction of more and more real-time monitoring systems, better mission profile data is expected to be available in various kinds of power electronic systems (e.g. PV inverters) [17]. This offers the possibilities to predict the lifetime of a certain inverter more accurately and provides possible estimation of energy production from PV power systems in certain applications. However, the solar irradiance together with the ambient temperature is various in different sites and in different seasons, where the PV inverter efficiency changes. It is necessary to investigate the transformerless inverters not only in a short-term but also in a long-term duration in such a way to predict the PV energy production and the inverter lifetime. Hence, a mission profile based multi-disciplinary evaluation method for single-phase transformerless PV systems is proposed. The analysis procedure of this method is shown in Fig. 1.

In the proposed evaluation method, the mission profiles - solar irradiance and ambient temperature (yearly data, monthly data and/or daily data) are taken as the input variables. The selected different transformerless inverter topologies are simulated in PLECS based on the thermal model shown in Fig. 1, which is also presented in details in § III. As it is shown in Fig. 1, the loss distribution in the power

devices and the junction temperature of the power modules, including mean/max junction temperature ($T_{jmax}$) and temperature cycling ($\Delta T_j$), can be obtained as the outputs of this proposed analysis method. Based on the resultant total losses and the thermal behavior, the energy production and the lifetime of a certain transformerless inverter can be obtained. Then, a benchmarking of the three topologies could be done in terms of efficiency, energy production and reliability.

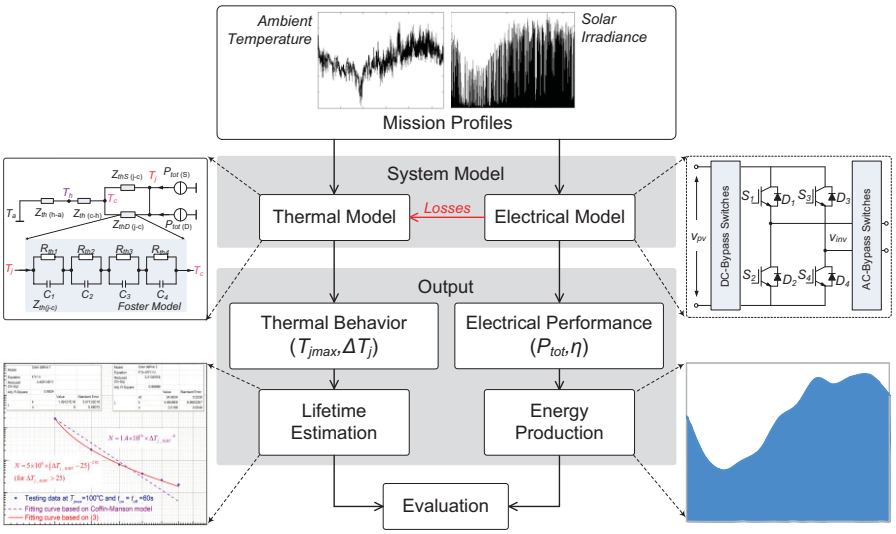


Fig. 1: Proposed mission profile based multi-disciplinary analysis method of single-phase transformerless PV inverters.

## Modelling of Single-Phase Transformerless Inverters

The proposed transformerless inverter topologies in the literature [8]-[15] are based on the traditional full-bridge inverter, which is shown in Fig. 2. As it is mentioned previously, the transformerless inverters should avoid the leakage current generation due to the lack of galvanic isolation. The leakage current is also known as a common-mode current. Thus, the goal of the transformerless inverters is to generate no varying Common-Mode Voltage (CMV, $V_{AB}$) in order to avoid leakage current.

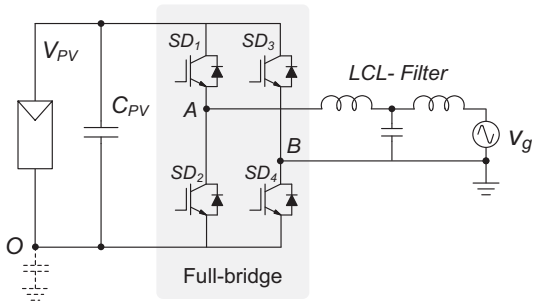


Fig. 2: Single-phase full-bridge grid-connected PV system with *LCL*-filter.

### Mainstream Transformerless Inverter Topologies

The elimination of leakage current can be achieved by disconnecting the PV panels from the inverter or by providing AC bypass with additional power devices. For example, the FB-DCBP (see Fig. 3(a)) patented by Ingeteam [12] can disconnect the PV panels from the inverter when the zero voltage state is applied to the grid; while the HERIC inverter (see Fig. 3(b)) by Sunways [13] adds a bypass path at the AC-side using two switching devices. The topologies in Fig. 2 and Fig. 3 have high efficiency due to no reactive power exchange between the *LCL*-filter and the DC-link capacitor $C_{PV}$ ($C_{PV1}$ and $C_{PV2}$) during zero voltage, which prevents the generation of varying common-mode voltage. This could be an inspiration to improve these topologies or to develop new topologies with high efficiency, such as the H5 inverter patented by SMA [14], the FB-ZVR inverter proposed in [15] and the REFU inverter developed by Refu Solar [8]. All these topologies require additional switching devices to realize the

disconnection, leading to a redistribution of power losses on the switching devices. Therefore, it may be a challenge on lifetime of those inverters due to increased complexity and redistributed power losses.

The full-bridge inverter with bipolar modulation is another solution to the leakage current elimination for full-bridge transformerless inverter. However, the test results shown in [12] and [15] reveal that the FB transformerless inverter has lower efficiency than that of FB-DCBP and HERIC. Moreover, the efficiencies of these inverters are solar irradiance (PV input power) dependent. In this paper, the FB inverter with bipolar modulation, the FB-DCBP inverter and the HERIC inverter are selected as the candidates for single-phase applications to be considered in terms of reliability.

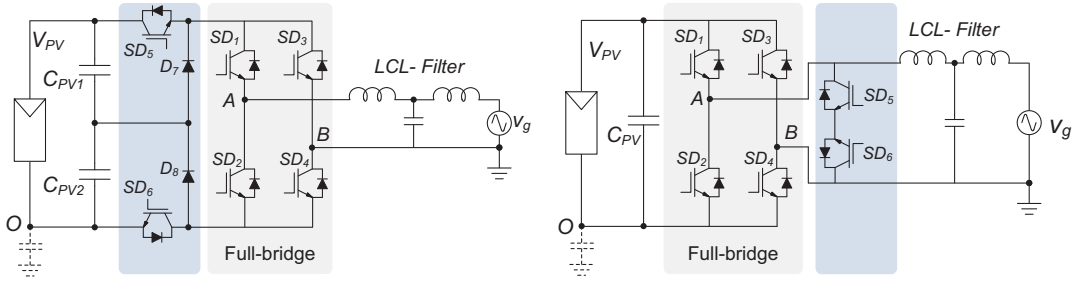


Fig. 3: Two grid-connected transformerless PV systems with *LCL*-filter.

## Thermal Model of IGBT Power Module

As it is shown in Fig. 1, the electrical performance (electrical model) of a power device is linked with its thermal behavior (thermal model) through the power losses on the device. The power losses, mainly including switching losses and conduction losses, will cause temperature rise at a certain point (e.g. the junction inside the device) because of thermal impedances. It has been observed that the junction temperature of the IGBT module is one of the most critical parameters for the lifetime estimation [17]-[19]. Thus, an accurate thermal model will be beneficial to the junction temperature estimation, and therefore to the lifetime prediction based on mission profiles.

The relationship between the power losses and the junction temperature can be modeled as shown in Fig. 4, and it can also be expressed as,

$$\begin{aligned} T_{j(S/D)}(t) &= P_{tot(S/D)}(t) Z_{th(S/D)(j-c)}(t) + T_c(t) \\ &= P_{tot(S/D)}(t) Z_{th(S/D)(j-c)}(t) + \left[ P_{totS}(t) + P_{totD}(t) \right] \cdot \left[ Z_{th(c-h)}(t) + Z_{th(h-a)}(t) \right] + T_a(t) \end{aligned} \tag{1}$$

in which,

$T_{j(S/D)}$ is the IGBT/diode junction temperature,
$P_{tot(S/D)}$ is the IGBT/diode total losses,
$Z_{th(S/D)(j-c)}$ is the thermal impedance from junction to case,
$Z_{th(c-h)}$ is the thermal impedance from case to heatsink,
$Z_{th(h-a)}$ is the thermal impedance from heatsink to ambient,
$T_c$ is the case temperature,
$S$ represents the IGBT and $D$ denotes the diode.

The thermal impedance from junction to case ($Z_{th(S/D)(j-c)}$) can be modelled as a physical-material-based Cauer RC network, which is a realistic representation, being more accurate to reflect the thermal transient behavior of an IGBT module [35]. However, the Cauer model requires in-depth material level information which is usually not available for power electronics designers. Thus, normally, the Cauer model is converted into a Foster model, of which the thermal parameters can be found in the datasheets. As it is shown in Fig. 4, the analytical function of the thermal impedance can be described as [36],

$$Z_{th(j-c)}(t) = \sum_{i}^{n} R_{thi} \left( 1 - e^{-t/\tau_i} \right). \tag{2}$$

According to (1) and (2), it is illustrated that the steady-state mean value ($t \rightarrow \infty$) of the junction temperature is dependent on the thermal resistance $R_{thi}$; while the dynamic behavior of the junction temperature is affected mainly by the thermal capacitance $C_i$ (time constant $\tau_i = C_i R_{thi}$). Moreover, the case temperature ($T_c$) has a much slower dynamic response than that of junction temperature ($T_j$) due to much larger time-constants of the thermal impedances ($Z_{th(c-h)}$ and $Z_{th(h-a)}$) [28], [36].

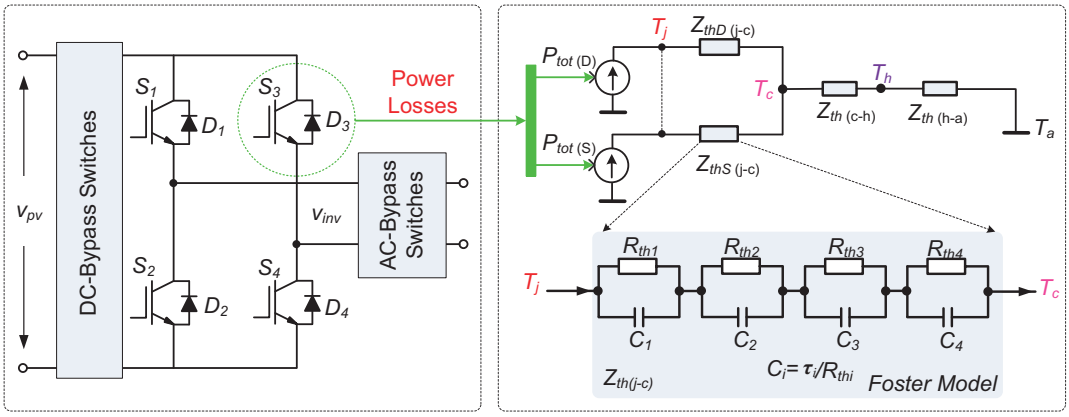


Electrical Model (Transformerless Inverters) Thermal Model for a Single Device

Fig. 4: Thermal model for a single device of the transformerless inverters [35]: $T_j$ – junction temperature, $T_c$ – case temperature, $T_h$ – heat-sink temperature, $T_a$ – ambient temperature.

## System Parameters and Mission Profiles

The 600V/50A IGBT module from a leading manufacturer has been selected as the power devices in the potential transformerless topologies. The PV array consists of 46 BP 365 PV modules (2 strings, 23 modules of each string), being the rated maximum power of 2990 W and the nominal voltage of 405 V at maximum power point under standard test conditions (25 °C, 1000 W/m$^2$). The thermal parameters in Fig. 4 can be found in the datasheets as listed in Table I. As it is discussed in the last paragraph, $Z_{(c-h)}$ and $Z_{(h-a)}$ have very large time-constants. Thus, for a time-effective simulation, the thermal capacitances in $Z_{(c-h)}$ and $Z_{(h-a)}$ are neglected since they have insignificant impact on the steady-state case temperature. The efficiency of Maximum Power Point Tracking (MPPT) is assumed to be 99%. Based on the maximum power of the PV array under different ambient temperatures shown in Fig. 5, three PV systems are simulated in order to obtain the corresponding output functions of solar irradiance and ambient temperature ($g_1$ and $g_2$) by means of curve-fitting. Fig. 6 illustrates the realization procedure of the method. Then, the selected inverters can be evaluated with yearly mission profiles.

For a long-term duration simulation, the proposed method can be used to evaluate the losses in a transformerless inverter, to compare the energy production of different transformerless inverters and to estimate the lifetime, as it is shown in Fig. 6. For a short-term application, the extreme solar irradiance change or temperature change (e.g. cloudy day) may directly introduce failures of the power devices in a transformerless inverter. Moreover, under a constant solar irradiance and ambient temperature condition, the junction temperature cycling and the power losses distribution, are also different in various transformerless topologies. Those can also be studied using the proposed method.

**Table I: Thermal parameters for a 600V/50A IGBT module.**

| Impedance | | $Z_{th(j-c)}$ | | | |
|---|---|---|---|---|---|
| $i$ | | 1 | 2 | 3 | 4 |
| IGBT | $R_{thi}$ (K/W) | 0.074 | 0.173 | 0.526 | 0.527 |
| | $\tau_i$ (s) | 0.0005 | 0.005 | 0.05 | 0.2 |
| Diode | $R_{thi}$ (K/W) | 0.123 | 0.264 | 0.594 | 0.468 |
| | $\tau_i$ (s) | 0.0005 | 0.005 | 0.05 | 0.2 |

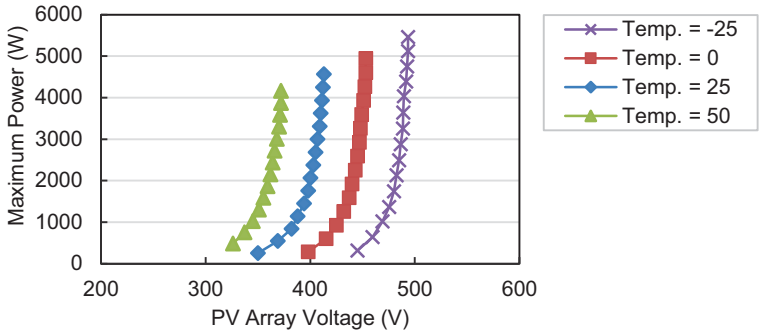


Fig. 5: Maximum output power of the PV array and the corresponding voltages under different ambient temperatures (°C).

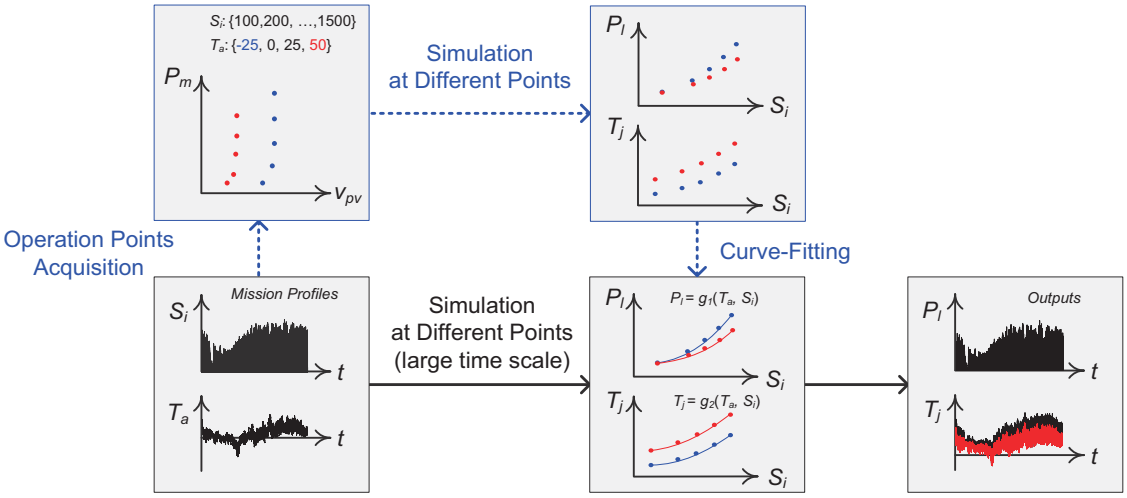


Fig. 6: Block diagram of the evaluation method for considering mission profiles: $P_m$ – PV maximum output power, $V_{pv}$ – PV voltage, $S_i$ – solar irradiance level, $T_a$ – ambient temperature, $P_l$ – total power losses on the switching device, $T_j$ – junction temperature.

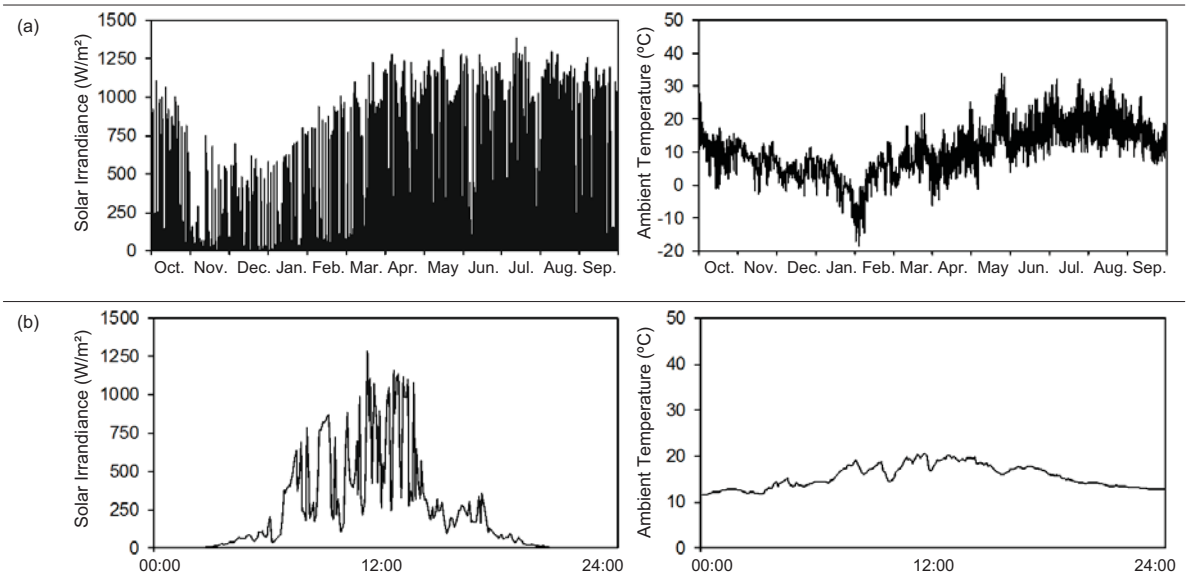


Fig. 7: Mission profiles from recorded data (5 minutes per sampling data) at Aalborg University: (a) yearly profiles from October 2011 to September 2012 and (b) a daily mission profile (cloudy day).

As it is shown in Fig. 6, in order to acquire the output functions of mission profiles, these selected mainstream transformerless inverters have firstly been evaluated under constant conditions. The ambient temperature range is -25 °C to 50 °C, and the solar irradiance changes from 100 W/m$^2$ to 1500 W/m$^2$.

These tests under the constant condition are also utilized to evaluate the static performance of the selected PV inverters under a certain condition, for example the power losses distribution and the thermal distribution in the transformerless topologies. Then, based on the output functions, the transformerless topologies have been simulated in terms of power losses and junction temperature behaviors under recorded mission profiles – yearly data and daily data, which are shown in Fig. 7, in order to evaluate the lifetime based on rain-flow analysis [17]-[19], [32]. The simulations have been carried out in MATLAB based on the PLECS Blockset in Simulink.

## Loss Distributions and Thermal Behaviors

The loss and thermal distributions in the power modules of the selected inverters under a constant condition (DC voltage 400 V, 50 °C ambient temperature, 1000 W/m$^2$ solar irradiance) are shown in Fig. 8 and Fig. 9 respectively. It can be seen from Fig. 8 that the loss distributions in the power devices are quite different among these three transformerless PV inverters, which illustrates why the efficiency of the transformerless inverters is different. The total power device losses of the HERIC inverter are the lowest among three transformerless inverters under a constant input power and constant ambient condition (solar irradiation and ambient temperature). It means the efficiency of the HERIC inverter is the highest. However, it might not be the same case when the mission profiles are taken into consideration.

Regarding the thermal stresses on the power devices, Fig. 9 demonstrates that the mean junction temperatures of the power devices of the HERIC transformerless topology are significantly lower than the other two topologies and thus it shows the most potential to further reduce the current rating and cost of the power devices. It is shown in Fig. 9(b) that the additional power devices are the most stressful ones in the FB-DCBP transformerless inverter. Thus, the reliability of this inverter is a challenge. Meanwhile, it reveals in Fig. 9(c) that the main switches of HERIC topology has higher junction temperature and swings than that of FB-DCBP and the auxiliary two switches have lower junction temperature and lower temperature swings.

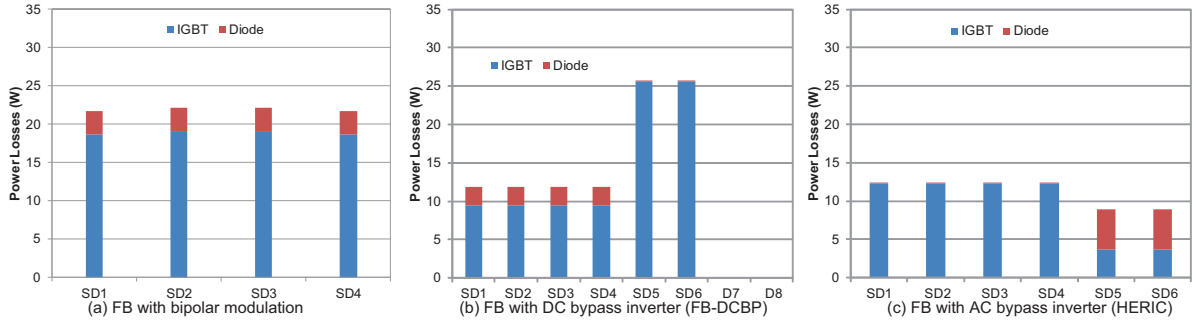


Fig. 8: Loss distribution in the device for three transformerless PV inverters with 3 kW nominal power under constant test condition (SD: IGBT+Diode, D: Diode).

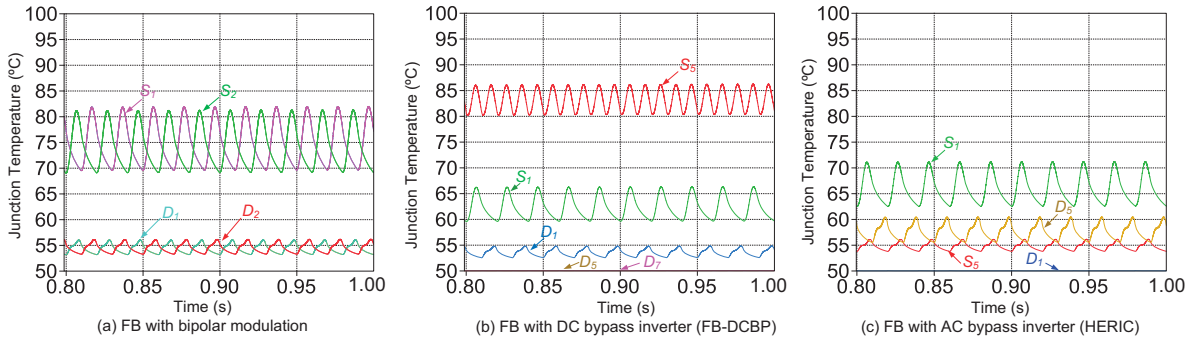


Fig. 9: Thermal distribution in the device for three transformerless PV inverters with 3 kW nominal power under constant test condition (S: IGBT, D: Diode).

In order to analyze the lifetime of selected transformerless inverters, the systems are tested using the proposed approach with a yearly mission profile and a daily mission profile. The results are shown in

Fig. 10 and Fig. 11 respectively. It can be concluded from Fig. 10 that HERIC transformerless inverter has reduced power losses on IGBTs and diodes compared to the other two topologies. Thus, if the HERIC inverter is adopted in a certain application, more energy will be produced in contrast to the case when the other two inverters are utilized.

As it is also discussed previously, the additional power devices in a transformerless PV inverter will introduce the redistribution of power losses, and thus lead to a redistributed thermal profile. It is seen from Fig. 9(b) and Fig. 11, although the thermal stress on the four power switches of the FB-DCBP transformerless inverter ($SD_1$~$SD_4$ in Fig. 3(a)) are reduced compared to that of the FB inverter with bipolar modulation, the thermal stress on the additional devices ($SD_5$~$SD_6$ in Fig. 3(a)) are much higher. Thus, in terms of reliability, the FB-DCBP inverter is not the best. As for the HERIC, it can maintain high efficiency with less thermal stress on the additional devices as shown in Fig. 11.

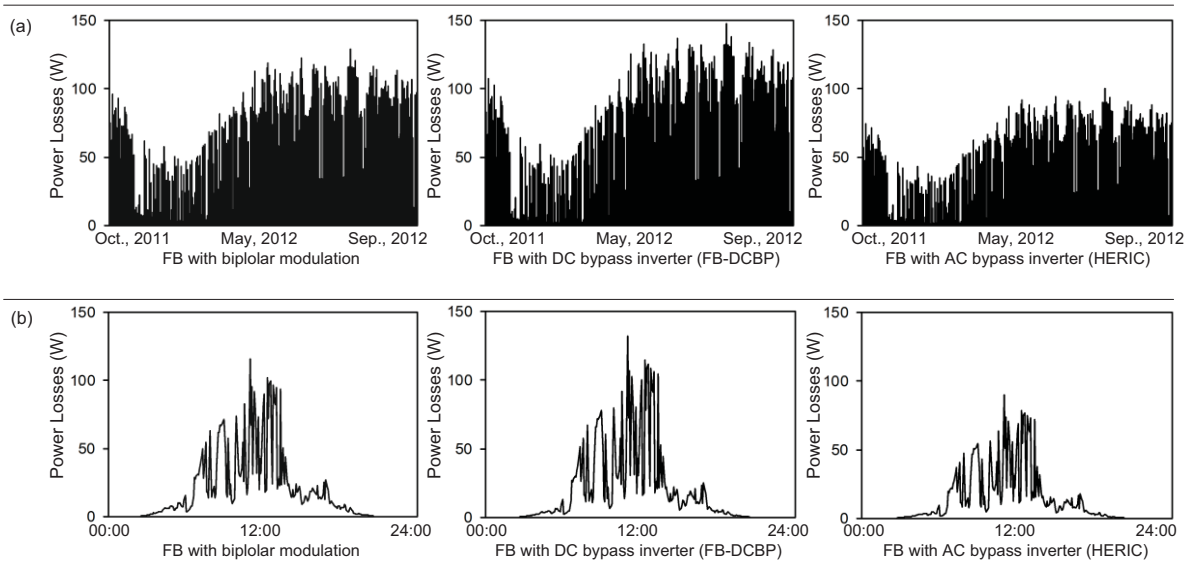


Fig. 10: Total power losses on the switching devices of the three transformerless PV inverters with (a) a yearly mission profile and (b) a daily mission profile.

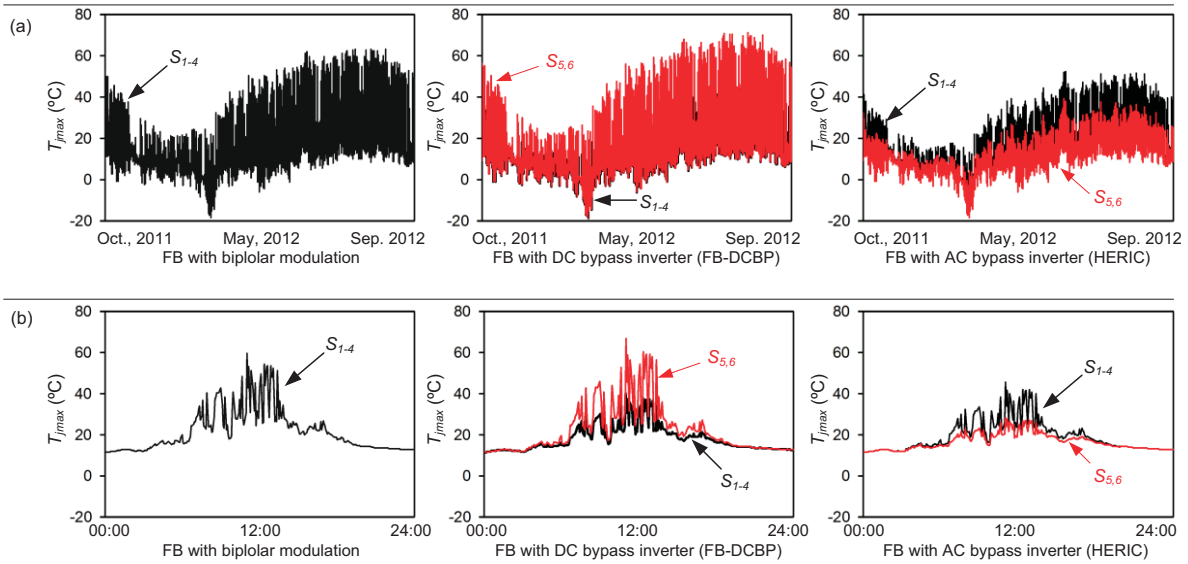


Fig. 11: IGBT maximum junction temperature ($T_{jmax}$) of the three transformerless PV inverters with (a) a yearly mission profile and (b) a daily mission profile.

## Lifetime Estimation

The well-known Coffin-Manson model [4], [20] or extended Coffin-Manson model [17] are applied for prediction of cycle-to-failure of IGBT modules due to temperature swings. Even though the parameters in those models are device dependent and their accurate values may not be available, the reliability performance of the switching devices in the three PV inverters under same environmental conditions could still be compared in a qualitative way from the thermal analysis results. One way to estimate or to compare the reliability is to do a rain-flow analysis, which has been used in recent studies [17]-[19], [32], [33]. Meaningful quantitative results could be obtained if the specific lifetime models are available and the impact of other stress factors (e.g. humidity and voltage) is also taken into account.

## Conclusion

In this paper, a mission profile based multi-disciplinary analysis of power modules in single-phase transformerless photovoltaic inverters has been proposed. It has been applied for the electrical-thermal analysis of the switching devices in three types of inverters, and the energy generation estimation of those inverters for a period of one-year operation based on the efficiencies. The electrical-thermal analysis under a long-term mission profile enables the comparative study of the reliability performance of different PV inverters in a qualitative or quantitative way, depending on the availability of the accurate lifetime models. Among the three analyzed inverters, the HERIC inverter has reduced power losses on the IGBT modules than that of the full-bridge transformerless inverter and the FB-DCBP inverter. Compared to the FB-DCBP inverter, HERIC inverter has much lower power losses on the auxiliary two switches used to realize galvanic isolation. The reduced power losses on the switching parts allow a better thermal performance, and therefore a better reliability performance of the HERIC inverter. The lifetime calculation of these topologies can be done by means of rain-flow analysis.

## References


[1] Blaabjerg F., Teodorescu R., Liserre M., and Timbus A.V.: Overview of control and grid synchronization for distributed power generation systems, IEEE Trans. Ind. Electron. vol. 53 no. 5, pp. 1398-1409, Oct. 2006.

[2] Kjaer S.B., Pedersen J.K., and Blaabjerg F.: A review of single-phase grid-connected inverters for photovoltaic modules, IEEE Trans. Ind. Appl. vol. 41 no. 5, pp. 1292-1306, Sept.-Oct. 2005.

[3] Golnas, A.: PV system reliability: an operator's perspective, IEEE Journal of Photovoltaics vol. 3 no. 1, pp. 416-421, Jan. 2013.

[4] Blaabjerg F., Ma K., and Zhou D.: Power electronics and reliability in renewable energy systems, IEEE ISIE 2012, pp. 19-30.

[5] Xue Y., Divya K.C., Griepentrog G., Liviu M., Suresh S., and Manjrekar M.: Towards next generation photovoltaic inverters, IEEE ECCE 2011, pp. 2467-2474.

[6] Kolar J.W., Krismer F., Lobsiger Y., Muhlethaler J., Nussbaumer T., and Minibock J.: Extreme efficiency power electronics, CIPS 2012, pp. 1-22.

[7] Meneses D., Blaabjerg F., Garcia O., and Cobos J.A.: Review and comparison of step-up transformerless topologies for photovoltaic AC-module application, IEEE Trans. Power Electron. vol. 28 no. 6, pp. 2649-2663, June 2013.

[8] Teodorescu R., Liserre M., and Rodriguez P.: Grid converters for photovoltaic and wind turbine systems, IEEE & Wiley, 2011.

[9] Zhang L., Sun K., Feng L., Wu H., and Xing Y.: A family of neutral point clamped full-bridge topologies for transformerless photovoltaic grid-tied inverters, IEEE Trans. Power Electron. vol. 28 no. 2, pp.730-739, Feb. 2013.

[10] Gu B., Dominic J., Lai J.-S., Chen C.-L., LaBella T., and Chen B.: High reliability and efficiency single-phase transformerless inverter for grid-connected photovoltaic systems, IEEE Trans. Power Electron. vol. 28 no. 5, pp. 2235-2245, May 2013.

[11] Gonzalez R., Gubia E., Lopez J., and Marroyo L.: Transformerless single-phase multilevel-based photovoltaic inverter, IEEE Trans. Ind. Electron. vol. 55 no. 7, pp. 2694-2702, July 2008.

[12] Gonzalez R., Lopez J., Sanchis P., and Marroyo L.: Transformerless inverter for single-phase photovoltaic systems, IEEE Trans. Power Electron. vol. 22 no. 2, pp. 693-697, March 2007.

[13] Schmidt H., Christoph S., and Ketterer J.: Current inverter for direct/alternating currents, has direct and alternating connections with an intermediate power store, a bridge circuit, rectifier diodes and a inductive choke, German Patent DE10 221 592 A1, Dec. 2003.

[14] Bremicker S., Greizer F., Hubler U., and Victor M.: Method of converting a direct current voltage from a source of direct current voltage, more specifically from a photovoltaic source of direct current voltage, into a alternating current voltage, US Patent, Publication Number: US 20050286281 A1, 2005.

[15] Kerekes T., Teodorescu R., Rodriguez P., Vazquez G., and Aldabas E.: A new high-efficiency single-phase transformerless PV inverter topology, IEEE Trans. Ind. Electron. vol. 58 no. 1, pp.184-191, Jan. 2011.

[16] Moore L.M. and Post H.N.: Five years of operating experience at a large, utility-scale photovoltaic generating plant, Journal of Prog. Photovolt: Res. Appl. vol. 16 no. 3, pp. 249-259, 2008.

[17] Wang H., Ma K., and Blaabjerg F.: Design for reliability of power electronic systems, IEEE IECON 2012, pp.33-44.

[18] Huang H. and Mawby P.A.: A lifetime estimation technique for voltage source inverters, IEEE Trans. Power Electron. vol. 28 no. 8, pp. 4113-4119, Aug. 2013.

[19] Wang H., Liserre M. and Blaabjerg F.: Toward reliable power electronics - challenges, design tools and opportunities, IEEE Industrial Electronics Magazine, in press, 2013.

[20] Ma K. and Blaabjerg F.: Multilevel converters for 10 MW wind turbines, EPE 2011, pp.1-10.

[21] Petrone G., Spagnuolo G., Teodorescu R., Veerachary M., and Vitelli M.: Reliability issues in photovoltaic power processing systems, IEEE Trans. Ind. Electron. vol. 55 no. 7, pp. 2569-2580, July 2008.

[22] Koutroulis E. and Blaabjerg F.: Design optimization of transformerless grid-connected PV inverters including reliability, IEEE Trans. Power Electron. vol. 28 no. 1, pp. 325-335, Jan. 2013.

[23] De Leon-Aldaco S.E., Calleja H., Chan F., Jimenez-Grajales H.R.: Effect of the mission profile on the reliability of a power converter aimed at photovoltaic applications—a case study, IEEE Trans. Power Electron. vol. 28 no. 6, pp. 2998-3007, June 2013.

[24] Shenoy P.S., Kim K.A., Johnson B.B., and Krein P.T.: Differential power processing for increased energy production and reliability of photovoltaic systems, IEEE Trans. Power Electron. vol. 28 no. 6, pp. 2968-2979, June 2013.

[25] Harb S. and Balog R.S.: Reliability of candidate photovoltaic module-integrated-inverter (PV-MII) topologies—a usage model approach, IEEE Trans. Power Electron. vol. 28 no. 6, pp. 3019-3027, June 2013.

[26] Blaabjerg F., Liserre M., and Ma K.: Power electronics converters for wind turbine systems, IEEE Trans. Ind. Appl. vol. 48 no. 2, pp.708-719, Mar.-Apr. 2012.

[27] Chan F. and Calleja H.: Reliability estimation of three single-phase topologies in grid-connected PV systems, IEEE Trans. Ind. Electron. vol. 58 no. 7, pp. 2683-2689, July 2011.

[28] Ma K. and Blaabjerg F.: Modulation methods for neutral-point-clamped wind powerconverter achieving loss and thermal redistribution under low-voltage-ride-through, IEEE Trans. Ind. Electron., early access, 2013.

[29] McCluskey, P.: Reliability of power electronics under thermal loading, CIPS 2012, pp. 1-8.

[30] Burgos R., Chen G., Wang F., Boroyevich D., Odendaal W.G., and Van Wyk J.D.: Reliability-oriented design of three-phase power converters for aircraft applications, IEEE Trans. Aero. and Electron. Sys. vol. 48 no. 2, pp. 1249-1263, Apr. 2012.

[31] Yang Y., Wang H., and Blaabjerg F.: thermal optimized operation of the single-phase full-bridge PV inverter under low voltage ride-through mode, PCIM Europe 2013, pp. 1055-1062, May 2013.

[32] Musallam, M. and Johnson, C.M.: An efficient implementation of the rainflow counting algorithm for life consumption estimation, IEEE Trans. Reliability, vol. 61, no .4, pp. 978-986, Dec. 2012.

[33] Bryant, A.T., Mawby, P.A., Palmer, P.R., Santi, E., and Hudgins, J.L.: Exploration of power device reliability using compact device models and fast electrothermal simulation, IEEE Trans. Ind. Appl. vol. 44 no. 3, pp. 894-903, May/June 2008.

[34] Busca C., Teodorescu R., Blaabjerg F., Munk-Nielsen S., Helle L., Abeyasekera T., and Rodriguez P.: An overview of the reliability prediction related aspects of high power IGBTs in wind power applications, Journal of Microelectronics Reliability vol. 51 no. 9-11 , pp. 1903-1907, 2011.

[35] Wintrich A., Nicolai U., Tursky W., and Reimann T.: Application manual power semiconductors, Nuremberg: ISLE Verlag, 2011.

[36] ABB: Application Note: Thermal design and temperature ratings of IGBT modules, [Online], Oct. 2011. Available: http://www.abb.com/semiconductors.